Dear Referee #2,

Thank you for your valuable suggestions and I have already revised the article according to your suggestions. The following are a few answers to some questions.

General Comments:

(1) "The authors point to the possibility for glacier surging and/or increases in precipitation to explain their observations of advancing glacier (Page 11, Lines 20-21) and thickening at glacier termini (Page 12, Lines 27-28). This should be expanded: is there any evidence of glacier surging in the region, e.g. from glacier morphological features and patterns? Regarding precipitation, the authors analyze a gridded climate product that shows a mix of increase and decrease in precipitation across the region, but they do not link these results to the inferences about advancing/thickening glaciers. This could be explored further by looking at trends in the accumulation area stake mass balance datasets and exploring more precipitation station data, including a consideration of solid versus liquid precipitation. "

Answer: I have already provided more discussion for advanced glaciers, and we found that advance of individual glaciers resulted from the increase of high precipitation.

"For advancing glaciers the mean size is about 0.51 km^2, mean surface slope about 27.9 º; most have an S or SW aspect, and a mean accumulation area ratio (AAR) of 51. Previous studies also found advancing glaciers in the Kangri Karpo (Liu et al., 2006; Shi et al., 2006). Comparing the CGI2 and GAMDAM inventories, the location of most glacier termini in 2000 are very close to those in 2014, indicating that the advance mainly occured before 2000. Unfortunately, due to location and climatic features, most Landsat MSS/TM image quality was too low to identify the snouts. Fortunately, two Landsat TM scenes (LT51340401994189BKT00 and LT51340401988301BJC00) did have enough quality to be used. Comparing the Landsat image of the terminus of Glacier 5O282B0111 (Fig. 3B), it could be determined that the advance occurred mainly before 1988 after which time the glacier retreated continuously (Fig. 7), and was likely due to increased precipitation in the 1980s (Shi et al., 2006). Annual precipitation data for 1980–2012 from the three nearest meteorological stations (Bomi, Zuogong and Zayu), indicated that the maximum precipitation was 1.3 times the mean precipitaion in the decade (1153 mm in 1988 vs. 891 mm) at Bomi (29°52′N, 95°46′E, 2736 m a.s.l.). At Zuogong (29 °40′N, 97 °50′E, 3780 m a.s.l.) the maximum precipitation was 1.5 times the mean (683 mm in 1987 vs. 405 mm), while at Zayu (28 °39′N, 97 °28′E, 2423 m a.s.l.) it was 1.4 times the mean (1091 mm in 1988 vs. 792 mm). Assuming variations in precipitation at the high-elevation glacier areas reflect those of the three nearest meteorological stations, the increased accumulation could certainly have influenced terminus activity. In complex terrain the accumulation distribution varies greatly so the response of glaciers may differ; some individual glaciers did advance between 1980 and 1988."

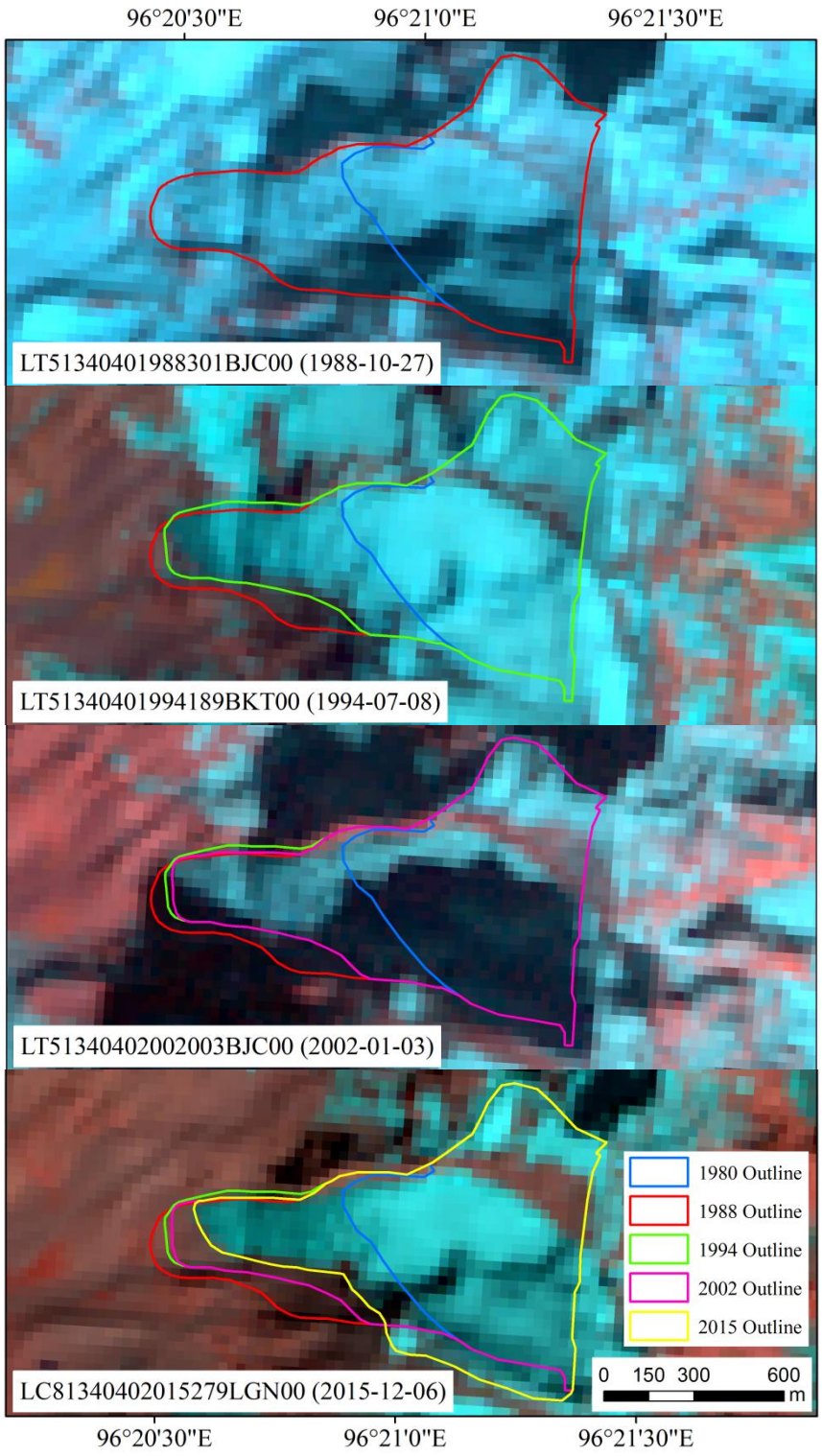

Figure 7. Terminus changes of Glacier 5O282B0111 from 1980 – 2015.

(2) “The authors make inferences about climate controls on the regional glacier mass loss on page 12-13 that are poorly supported.”

Answer: I have already provided more discussion for climate controls on the regional glacier mass loss, and we found that climate warming is the primary control on the regional mass balance.

“Rainfall increased slightly in the Kangri Karpo during 1980–2012. This increase in precipitation resulted in more glacier accumulation yet the glaciers experienced an intense mass deficit. Other factors must be playing a more important role in this deficit. In the case of temperature, warming was present in the Kangri Karpo during 1980–2012. Meteorological sration records indicate that average air temperature increased in the Kangri Karpo Mountains more than 0.2 ℃ per decade (with confidence level <0.05), higher than the rate of warming in global (0.12 ℃ per decade, 1951–2012). The rate of warming on the northern slope is slightly larger than that on the southern slope. Meteorological sration records showed that average air temperature increased at 0.27 ℃ per decade and 0.25 ℃ per decade in Bomi and Zuogong station, higher than Zayu station slightly (0.2 ℃ per decade). While a small warming rate was present from 1980–2000 it increased to large warming rate thereafter. This is consistent with how the glaciers have changed. In the Kangri Karpo they have experienced a substantial area reduction and mass deficit. The mean mass deficit in drainage basin 5O282B (on the northern slope) was larger than that in drainage basin 5O291B (on the southern slope) during 1980–2014. Furthermore, the rate of glacier shrinkage and mass loss from 1980–2000 was less than from 2000–2015. Thus, the changes leading to glacier wastage in the Kangri Karpo can be attributed to climate warming. ”

Specific Comments:

“Page 2, Lines 16-22: This paragraph is confusing: how was mass deficit established?”

Answer: Thank you for your suggestion and I have already revised this paragraph.

“While previous studies agreed that glaciers in the Kangri Karpo were losing mass, the results did differ from each other. Using SRTM and SPOT5 DEMs (24 November 2011), Gardelle et al. (2013) found a mean thinning of 0.39 ± 0.16 m a^{-1}, whereas Kääb et al. (2015), Neckel et al. (2014) and Gardner et al. (2013), using ICESat and SRTM, recorded thinning of 1.34 ± 0.29 m a^{-1}, 0.81 ± 0.32 m a^{-1} and 0.30 ± 0.13 m a^{-1} from 2003–2009, respectively.”

“Page 3, Line 33: Generally, elevations derived from aerial photography over high elevation, snow covered regions have larger uncertainties due to poor contrast in the imagery. Do the authors have any additional information on this?”

Answer: More information was added in this paragraph.

“According to the photogrammetric Chinese National Standard (2008) issued by the Standardization Administration of the People’s Republic of China, the nominal vertical accuracy of these topographic maps was within 3-5 m for flat and hilly areas (with slopes of < 2 ° and 2-6 °, respectively) and within 8-14 m for the mountainsides and high mountain areas (with slope of

6-25 ° and >25 °, respectively). Since the slopes of the most of the glacierized areas in the Kangri Karpo were gentle (~19 °), the vertical accuracy of the TOPO DEM on the glaciers is better than 9 m."

"Page 5, Line 18: Is it problematic to rely on Google Earth imagery, since it is not possible to know the dates of the images?"

Answer: Google Earth imagery did not be used in this study. The high-resolution images of Google Earth™ were used to validate the accuracy of the glacier delineation methods in the second Chinese glacier inventory. Google Earth™ images were captured for seven randomly selected regions, where higher-resolution images in Google Earth™ and nearly simultaneous Landsat images are available (Guo et al., 2015). Due to the same data sources and method of glacier inventory between this study and the second Chinese glacier inventory, the study of Guo et al. (2015) was cited to validate the accuracy of the glacier delineation methods in this study.

"Page 5, Line 31: I am unable to access the Yao et al reference: what is a "glacier axis concept"?"

Answer: Thank you for your suggestion and more information about glacier axis concept was added.

"In this study, a new method, based on an axis concept derived from the glacier's shape, was applied; requiring only the glacier outline and the DEM as input (Yao et al., 2015). The glacier-axis concept assumes the main direction of any given glacier can be defined as a curved line. The glacier outline is divided initially into two curved lines based on its highest and its lowest elevation. Using these, the glacier polygon is then divided by Euclidean distance into two regions. The common boundary of these two regions is the glacier axis or glacier centerline."

"Page 6, Lines 1-27: This paragraph is very hard to decipher, especially for a non-expert in SAR processing. Improvement of the grammar should help in this regard."

Answer: I have already revised this paragraph, and the SAR processing was introduced in detail.
"The TerraSAR-X/TanDEM-X acquisitions were processed by differential SAR interferometry (DInSAR) (Neckel et al., 2013) using GAMMA SAR and interferometric processing software (Werner et al., 2000).

The interferometric phase of the single-pass TerraSAR-X/TanDEM-X interferogram can be described by

$$\Delta_{\phi TSX/TDX} = \Delta_{\phi orbit} + \Delta_{\phi topo} + \Delta_{\phi atm} + \Delta_{\phi scat} \quad (1)$$

where $\Delta_{\phi TSX/TDX}$ is the phase difference of phases ϕTSX and ϕTDX simultaneously acquired by TerraSAR-X and TanDEM-X, $\Delta_{\phi orbit}$ is that from the different acquisition geometry of the SAR sensors, and $\Delta_{\phi topo}$ from topography. $\Delta_{\phi atm}$ and $\Delta_{\phi scat}$ are the phase differences introduced by atmospheric conditions and different scattering on the ground. As the TerraSAR-X/TanDEM-X

data were acquired simultaneously, the same atmospheric conditions and scattering could be assumed for both SAR antennas, thus setting $\Delta_{\emptyset\mathrm{atm}}$ and $\Delta_{\emptyset\mathrm{scat}}$ in Eq. (1) to zero. $\Delta_{\emptyset\mathrm{orbit}}$ was removed from the interferogram by subtracting a simulated flat-earth phase trend (Rosen et al., 2000).

The DInSAR approach can be described by

$$\Delta_{\emptyset\mathrm{diff}} = \Delta_{\emptyset\mathrm{TSX/TDX}} - \Delta_{\emptyset\mathrm{SRTM-C}} \quad (2)$$

where $\Delta_{\emptyset\mathrm{SRTM-C}}$ is the February 2000 SRTM-C interferometric phase. Lacking the raw interferometric data, $\Delta_{\emptyset\mathrm{SRTM-C}}$ was simulated from SRTM-C DEM data using the satellite geometry and a baseline model of the TerraSAR-X/TanDEM-X pass. Thus the differential phase $\Delta_{\emptyset\mathrm{diff}}$ is based solely on changes in $\Delta_{\emptyset\mathrm{topo}}$ between data acquisitions (Neckel et al., 2013).

To improve the phase-unwrapping procedure and minimize errors, the unfilled, finished, SRTM C-band DEM was employed. Before generating the differential interferogram, precise horizontal offset registration and fitting between the SRTM C-band DEM and the TerraSAR-X/TanDEM-X acquisitions is required. Based on the relation between the map coordinates of the SRTM C-band DEM segment covering the TerraSAR-X/TanDEM-X master file, and the SAR geometry of the respective master file, an initial lookup table was calculated. While the areas of radar shadows and layover in the TerraSAR-X/TanDEM-X interferogram would introduce gaps in the lookup table, a method of linear interpolation between the gap edges in each line of the lookup table was used to fill these gaps. The offsets between the master scene and the simulated intensity of the SRTM C-band DEM, were calculated using cross-correlation optimization of the simulated SAR images employing *GAMMA's offset_pwrm* module. The horizontal registration and geocoding lookup table were refined by these offsets. The SRTM C-band DEM was translated from geographic coordinates into SAR coordinates via the refined geocoding lookup table, and conversely, the final difference map was translated from SAR coordinates into geographic coordinates. Then a differential interferogram was generated by the TerraSAR-X/TanDEM-X interferogram and the simulated phase of the co-registered SRTM C-band DEM. An adaptive filtering approach was used to filter the differential interferogram (Goldstein and Werner, 1998). *GAMMA's* minimum cost flow (MCF) algorithm was then employed to unwrap the flattened differential interferogram. According to the computed phase-to-height sensitivity and select ground-control points (GCPs) from respective off-glacier pixel locations in the SRTM C-band DEM, the unwrapped differential phase was converted to absolute differential heights. While, a residual not covered by the baseline refinement would exist it can be regarded as a linear trend estimated by a two-dimensional first-order polynomial fit in off-glacier regions. The linear trend and a constant vertical offset were removed from the maps of absolute differential heights. Finally, the resulting datasets were translated to a metric cartographic coordinate system with 30 m $\times$ 30 m pixel spacing (Neckel et al., 2013). The same DInSAR method was employed to acquire the glacier elevation change from 1980–2014 with the data from the TOPO DEM and TerraSAR-X/TanDEM-X acquisitions."

"Page 7, line 12: Specify how this density uncertainty value was chosen."

Answer: The value of density uncertainty was chosen by previous studies of Gardner et al. (2013) and Neckel et al. (2015).

"Page 8, Lines 36-43: It is a bit difficult reading through all of these numbers. Could the authors condense this into a box plot or something similar?"

Answer: Thank you for your suggestion. There have Table 5 and Table 6 that can introduce the length changes of advanced glaciers and retreated glaciers clearly.

"Page 9, Lines 34-37: more information on the percentage of debris cover on individual glaciers and over the entire region would be valuable."

Answer: Thank you for your suggestion and more information about debris cover was added in this paragraph.

"A marked thickening (elevation increase) was observed at the termini of two glaciers (5O291B0113 and 5O291B0117) on the southern slope of the Kangri Karpo (Fig. 6C). Substantial debris-cover of 3.79 km^2 and 3.70 km^2, accounts for 20.6% and 31.4% of their individual area and 69.4% and 63.3% of their length. The termini of these glaciers probably remained stable from October 1980 to October 2015 because of this debris cover."

"Page 10, Lines 29-32: How do these results reconcile with the findings of Liu et al., 2006, who found 40% of glaciers were advancing in the region between 1980 – 2001?"

Answer: The findings of Liu et al. (2006) and this study both resulted from Topographic Maps that generated from aerial photos acquired in October 1980. Glacier inventory in other mountains of western China, resulted from Topographic Maps, has fewer mistakes that fewer glacier outlines are not accurate. In order to improve the accuracy of glacier inventory in this study, aerial photographs was employed to check and revise glacier outlines that resulted from Topographic Maps. Hence, the results of this study are more reliable and more accurate.

"Page 12, Lines 11-12: It is unclear how these different thinning rates for debris versus clean ice were calculated? Were entire glaciers classified as debris covered, or specific elevation bands? If so, what was the threshold of debris required to classify it in the debris-covered category?"

Answer: Thank you for your suggestion. These different thinning rates for debris versus clean ice were calculated in specific elevation bands.

"Thinning was noticeably greater on the glacier debris-cover than the white ice in the 2800–5300 m a.s.l. altitude range from 1980–2014 (-0.99 $\pm$ 0.09 m a^{-1} vs. -0.89 $\pm$ 0.08 m w.e. a^{-1}) (Fig. 8). Clean-ice extended down to 2800 m a.s.l. whereas 5300 m a.s.l. was the highest altitude of the debris-covered region. The mass-loss patterns on a debris-covered tongue are complicated, with supraglacial lakes, ice cliffs and a heterogeneous debris cover, (Pellicciotti et al., 2015). Although it is generally believed that ablation rates are retarded with a thick debris-cover due to its insulation effect, some previous studies have found that ablation is greater when the debris is less

than a critical thickness (Nakawo and Young, 1981; Pu et al., 2003; Ye et al., 2015; Zhang et al., 2011; Zhang et al., 2016a). The situation of debris-covered regions at lower altitudes with higher temperatures, and the development of supraglacial lakes and ice cliffs, likely contributed to the larger mass loss in those regions (Benn et al., 2012; Sakai and Fujita, 2010).”

Best Regards,
Wu Kunpeng and other authors